

# AN ADAPTIVE ALGORITHM FOR SAMPLING TWO-DIMENSIONAL FIELDS USING MOBILE SENSORS

Huiyu Luo, Xiangming Kong, and Gregory Pottie

University of California, Los Angeles

## ABSTRACT

In this paper, we propose an adaptive algorithm for sampling and reconstructing two-dimensional fields using mobile sensors that can move to designated locations to collect measurements. During each step, the algorithm selects the most desirable sampling sites from a pool of site candidates based on a Bayesian framework. Simulations show that the algorithm works effectively.

**Index Terms**— Bayes procedures, Adaptive systems, Delaunay triangulation, Spline functions

## 1. INTRODUCTION

In this paper, we consider sampling two-dimensional fields using mobile sensors that can move to prescribed locations to collect samples, e.g. the Networked InfoMechanical System (NIMS) [1]. Equipped with mobility, a few sensors can carry out the task of collecting measurements within their patrol area, which would otherwise require a large number of static sensors. Moreover, mobile sensors are especially suited for observing heterogeneous and slowly time-varying phenomena owing to their ability to sample the field at arbitrary and adjustable density.

Traditional algorithms often begin with a panorama, then proceed to compress the complete set of data under some distortion constraint. For instance, image compression and the approach in [2] fall in this category. Here, the process is reversed. Unless the source is exhaustively sampled, which is prohibitively expensive, we possess only partial knowledge about the field. Hence, it is more appropriate to consider the probability of satisfying the fidelity constraint given the incomplete information at hand. New levels of confidence on achieving the fidelity goal can be gained by collecting more samples. Herein lies the compromise between our fidelity goal and the resource consumption. Furthermore, the heterogeneous nature of the field presents us the opportunity (challenge) of reaching a high confidence level efficiently.

In a mobile sampling system, major energy expenditure often results from sensor movement and sample collection.

This work is supported by the NSF grant CCR-0121778 and the NSF graduate fellowship.

Hence, the number of samples provides a first-order indication of energy expense. On the other hand, when the field varies slowly in time, using fewer samples to estimate a field snapshot leads to a faster and more accurate system. Hence, the goal here is to minimize the number of samples under a certain fidelity constraint.

In a sense, the sequential sampling process can be viewed as an optimal experimental design [3], in which the input variables (new sampling sites) of a series of tests (sample collection) are adjusted such that the system response (the field) is observed efficiently. [4] explores this idea in choosing optimal trajectories of moving sensors based on the Fisher information matrix. A sequential method for estimating discontinuities in curves and surfaces is discussed in [5]. However, these schemes are not readily applicable to distributed field reconstruction under fidelity constraints. [1] and [6] represent preliminary efforts on using mobile sensors to adaptively sample distributed phenomena. Recently, [7, 8] show that adaptive and nonadaptive methods result in the same error convergence rate for certain classes of functions. Yet, we still consider adaptive methods a competitive approach for several reasons. First, the methods are evaluated on a minimax criterion in [7, 8]. Second, even with the same convergence rate, the scaling factor may be different. Third, algorithm complexity is important too.

The rest of the paper is organized as follows. The adaptive algorithm is presented in Section 2, and simulation results are displayed in Section 3. Section 4 concludes the paper.

## 2. ADAPTIVE SAMPLING ALGORITHM

The block diagram of our adaptive algorithm is depicted in Fig. 1. We assume that a single mobile sensor is used. A pool of sampling candidates is maintained and updated each time

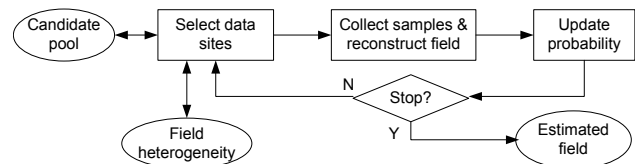


Fig. 1. The block diagram of the adaptive sampling algorithm.

a new sampling point is picked. A number of sites are picked from the pool based on a Bayesian framework. The sensor then moves to collect samples at these locations, and reconstructs the field. The probability of the newly reconstructed field satisfying the fidelity constraint is updated. The algorithm iterates until the confidence of meeting the fidelity constraint is high enough or the number of samples has reached a prescribed value.

## 2.1. Sampling Candidates

Given a set of points  $\mathcal{S}$ , a Delaunay tessellation  $\text{DT}(\mathcal{S})$  is obtained by connecting any two points  $p, q \in \mathcal{S}$  with a line segment if there exists a circle that passes through  $p, q$  and contains no other points of  $\mathcal{S}$ .  $\text{DT}(\mathcal{S})$  is the graph-theoretic dual of  $\text{V}(\mathcal{S})$ , the Voronoi diagram with respect to  $\mathcal{S}$  [9].

Denoting by  $\mathcal{S}_k$  the set of existing sampling sites at iteration  $k$  and  $N_k$  the size of  $\mathcal{S}_k$ , we construct  $\text{DT}(\mathcal{S}_k)$ , and use as site candidates the centers of Delaunay cells' circumcircles (Fig. 2). This choice has some nice properties. First, our scheme follows the maximin design [10] by placing potential sites at the centers of sampling gaps. Second, the total number of Delaunay cells is no more than  $(2N_k - 5)$ . Third, there are parallel algorithms that run in  $O(N_k \log N_k)$  time finding  $\text{DT}(\mathcal{S}_k)$  [9]. Moreover, incremental schemes that update the pool in the neighborhoods of newly added sites exist.

For the Delaunay cell corresponding to the  $m$ th candidate in  $\text{DT}(\mathcal{S}_k)$ , we define  $\mathcal{O}_m^k$  as its set of vertices, i.e. the sampling points that are closest to the  $m$ th candidate. Denoting by  $\mathcal{V}_j^k$  the Voronoi cell corresponding to the  $j$ th sampling site during iteration  $k$ , then the  $m$ th candidate at iteration  $k$  is also the common vertex of Voronoi cells  $\mathcal{V}_j^k$ ,  $j \in \mathcal{O}_m^k$ , which can be easily seen from Fig. 2.

## 2.2. Adaptive Sample Selection

### 2.2.1. Sample Selection

We consider the following distortion requirement:

$$\max_{(x,y) \in \text{Dom}} |f(x,y) - s(x,y)| \leq D_{\max}, \quad (1)$$

where  $\text{Dom}$  is the sampling domain, and  $f(x,y)$  and  $s(x,y)$  are the actual and reconstructed fields. We impose the error requirements on each Voronoi cell ( $\mathcal{V}_i^k$ ), and define:

$$U_i^k : \text{Distortion requirement is unsatisfied in } \mathcal{V}_i^k. \quad (2)$$

(1) is satisfied if (2) is false for all Voronoi cells.

When a sample is collected, besides being used to obtain a new field estimation, this sample also reveals important information on how well the previous estimation approximates  $f(x,y)$  in the vicinity of sampling site. We can define a test  $T_i^k$  for the sample taken at  $(x_i, y_i)$  during iteration  $k$ :

$$T_i^k = \begin{cases} \text{G} & \text{if } |s_k(x_i, y_i) - s_{k-1}(x_i, y_i)| > \epsilon, \\ \text{L} & \text{otherwise,} \end{cases}$$

where  $s_k(x,y)$  and  $s_{k-1}(x,y)$  are estimations at iteration  $k$  and  $k-1$  respectively, and  $\epsilon$  is set according to  $D_{\max}$ . Group the samples collected during one iteration, and accumulate all tests up to  $k$ . We have

$$T^k = \{T_1^k, \dots, T_n^k\}, \quad Z^k = \{T^k, T^{k-1}, \dots, T^1\},$$

where  $n$  is the number of samples taken in one iteration.

Due to insufficient knowledge about the field, we are generally not certain about whether the fidelity constraint is satisfied in  $\mathcal{V}_i^k$ . However, we can define  $P(U_i^k | Z^k)$ , the probability of  $U_i^k$  given all past tests. To continue sampling, new data sites need to be picked from the candidate pool. Since each selected site creates a new Voronoi cell at the next iteration, it is natural to choose the site with the maximum  $P(U_i^{k+1} | Z^k)$  among all candidates. Supposing the cell  $\mathcal{V}_i^{k+1}$  corresponds to candidate  $m$  at iteration  $k$ , then  $\mathcal{V}_i^{k+1}$  overlaps with  $\mathcal{V}_j^k$ ,  $j \in \mathcal{O}_m^k$ , (recall that  $m$  is the common vertex of  $\mathcal{V}_j^k$ ,  $j \in \mathcal{O}_m^k$ ). Therefore, a weighted sum is used to estimate this probability:

$$P(U_i^{k+1} | Z^k) = \sum_{j \in \mathcal{O}_m^k} \mu_j P(U_j^k | Z^k). \quad (3)$$

The weight  $\mu_j$  characterizes the influence of  $\mathcal{V}_j^k$  on  $\mathcal{V}_i^{k+1}$ :

$$\sum_{j \in \mathcal{O}_m^k} \mu_j = 1 \quad \text{and} \quad \mu_j \propto (d_{j1} + d_{j2}) / r_j. \quad (4)$$

in which  $d_{j1}$ ,  $d_{j2}$ , and  $r_j$  are defined as in Fig. 2.

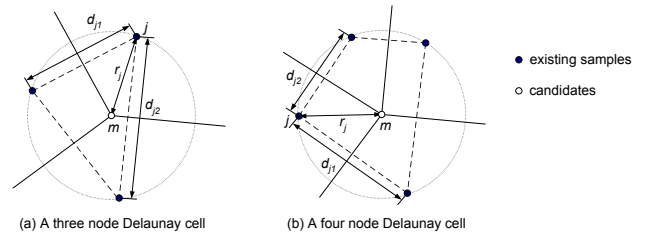


**Fig. 2.** Delaunay cells are enclosed by dashed lines. Solid lines are boundaries of Voronoi cells.

Once data sites are chosen, samples are collected, and the field is estimated. It remains to compute  $P(U_i^{k+1} | Z^{k+1})$  by assimilating the information revealed from  $T^{k+1}$ .

### 2.2.2. Probability Update

Based on the Bayesian framework, we have:

$$\begin{aligned} P(U_i^{k+1} | Z^{k+1}) &= P(U_i^{k+1} | T^{k+1}, Z^k) \\ &= \frac{P(T^{k+1} | Z^k, U_i^{k+1})}{P(T^{k+1} | Z^k)} P(U_i^{k+1} | Z^k) \end{aligned} \quad (5)$$

It is difficult to compute the exact value of each quantity in (5). Instead, we design schemes that approximate the procedure.

$P(U_i^{k+1}|Z^k)$  from (3) is used if  $\mathcal{V}_i^{k+1}$  corresponds to a sample collected at iteration  $k+1$ . Otherwise  $P(U_i^{k+1}|Z^k) = P(U_j^k|Z^k)$ , where  $\mathcal{V}_i^{k+1}$  contains the same data site as  $\mathcal{V}_j^k$ .

Literally,  $P(T^{k+1}|Z^k, U_i^{k+1})$  is the probability of  $T^{k+1}$  given  $Z^k$  and the knowledge that the fidelity constraint is unsatisfied in  $\mathcal{V}_i^{k+1}$ . If  $\mathcal{V}_i^{k+1}$  is far away from the sites sampled at iteration  $k+1$ , the status of  $\mathcal{V}_i^{k+1}$  exerts little influence on the outcome of  $T^{k+1}$ . Hence,  $P(T^{k+1}|Z^k, U_i^{k+1}) = P(T^{k+1}|Z^k)$ , and  $P(U_i^{k+1}|Z^{k+1}) = P(U_i^{k+1}|Z^k)$ , which implies that  $T^{k+1}$  sheds no information on Voronoi cells far away from the testing sites. Now, assume  $\mathcal{V}_i^{k+1}$  is near a sample collected during iteration  $k+1$  at candidate  $m$ , and  $T_m^{k+1}$  is the corresponding test. Fixing the values of the rest tests in  $T^{k+1}$ , we examine the effect of  $U_i^{k+1}$  on  $T_m^{k+1}$ . For simplicity, we keep only  $T_m^{k+1}$  in writing  $T^{k+1}$ . If  $\epsilon$  is properly set according to  $D_{\max}$ , we expect

$$P(T_m^{k+1} = \text{G}|Z^k, U_i^{k+1}) > P(T_m^{k+1} = \text{G}|Z^k);$$

$$P(T_m^{k+1} = \text{L}|Z^k, U_i^{k+1}) < P(T_m^{k+1} = \text{L}|Z^k).$$

We find the following scheme effective. Assuming  $m$  the candidate corresponding to  $T_m^{k+1}$ , if  $\mathcal{V}_i^{k+1}$  is created by  $m$ ,

$$P(U_i^{k+1}|Z^{k+1}) = \begin{cases} [P(U_i^{k+1}|Z^k)]^{\kappa_g} & \text{if } T_m^{k+1} = \text{G}; \\ [P(U_i^{k+1}|Z^k)]^{\kappa_l} & \text{else.} \end{cases} \quad (6)$$

If the data site of  $\mathcal{V}_i^{k+1}$  is inherited from  $\mathcal{V}_j^k$ ,  $j \in \mathcal{O}_m^k$ ,

$$P(U_i^{k+1}|Z^{k+1}) = \begin{cases} [P(U_j^k|Z^k)]^{\alpha_j} & \text{if } T_m^{k+1} = \text{G}; \\ [P(U_j^k|Z^k)]^{\beta_j} & \text{else,} \end{cases} \quad (7)$$

where  $\alpha_j = \kappa_g^{\mu_j}$  and  $\beta_j = \kappa_l^{\mu_j}$ . Otherwise,

$$P(U_i^{k+1}|Z^{k+1}) = P(U_j^k|Z^k). \quad (8)$$

Here,  $\kappa_g < 1$ ,  $\kappa_l > 1$  are parameters properly set according to  $\epsilon$  and  $D_{\max}$ . Using the same  $\kappa_g$  and  $\kappa_l$  for all tests implicitly assumes that cells are uniform. Thus a compensating factor is used to take into account cell area ( $\Delta_i$ ) and field roughness.

$$h_i = \left[ \left( \frac{\partial^2 s}{\partial x^2} \right)^2 + 2 \left( \frac{\partial^2 s}{\partial x \partial y} \right)^2 + \left( \frac{\partial^2 s}{\partial y^2} \right)^2 \right] \Delta_i.$$

### 2.3. Algorithm Implementation

Starting with a set of sampling sites and the initial field estimation. Set  $k = 1$ , and execute the following steps.

1. Compute  $P(U_i^{k+1}|Z^k)$  for all candidates using (3).
2. Calculate  $h_i$  and  $C_i^s = h_i P(U_i^{k+1}|Z^k)$ . Pick  $N$  candidates that maximizes  $C_i$ .
3. Collect samples at selected sites and reconstruct the field. Evaluate  $T^{k+1}$ , and update probabilities using (6), (7), and (8).

4. If  $P(U_i^{k+1}|Z^{k+1})$ ,  $i = 1, \dots, N_{k+1}$ , reach required values or enough samples have been collected, exit. Otherwise,  $k = k + 1$ , and go to step 1.

When multiple samples are collected during one iteration, the candidate pool and  $C_i$  is updated each time a data site is selected to avoid picking two sites too close to one another. We ignore noise in this paper, so the thin plate spline [11] is used to interpolate the field. If noise is to be considered, approximation, for instance, the smoothing spline [12], must be used for field reconstruction.

When  $P(U_i^k|Z^k)$  and field variation appear the same everywhere, the algorithm degenerates to a uniform sampling scheme that follows the maximin design to fill the space efficiently. On the other hand, the probability  $P(U_i^k|Z^k)$  will monotonically decrease when the tests in the neighborhood repeatedly result in L. Therefore, our algorithm is stable in that it will not keep sampling a region after the reconstructed field has reached the fidelity constraint.

In addition, we often have some knowledge about the field smoothness so that some cutoff rate can be specified as an upper bound on the spatial sampling density. This can result in considerable saving because otherwise we have to oversample in each cell to reach a high level of confidence on fidelity.

## 3. SIMULATIONS

We first describe a uniform sampling method that our adaptive algorithm will be compared with. A pool of sampling candidates is maintained as in section 2.1. At each step, the candidate with the maximum distance to existing samples is picked as the new site. This method follows the maximin design and tends to spread the sampling sites uniformly in space.

### 3.1. Sunlight field

The first simulation is based on the sunlight field under the forest canopy, which has long interested biologists due to their important role in plant growth [13]. The true sunlight field captured with a digital camera at the UCLA sunset canyon is depicted in Fig. 3(a). Field estimations reconstructed from

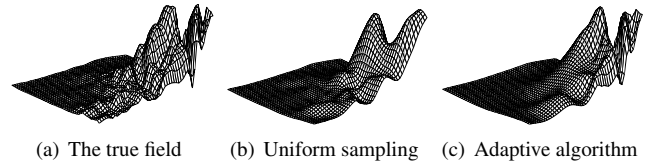


Fig. 3. The true and reconstructed fields.

102 samples collected using uniform and adaptive sampling methods are shown in Fig. 3(b) and 3(c). While Fig. 3(c) reasonably approximates the true field, Fig. 3(b) smears the cut in the corner badly. The sample distribution in Fig. 4 explains the difference: the uniform method distributes samples

uniformly in space; in contrast, the adaptive method focuses most samples in the region where field variation is high.

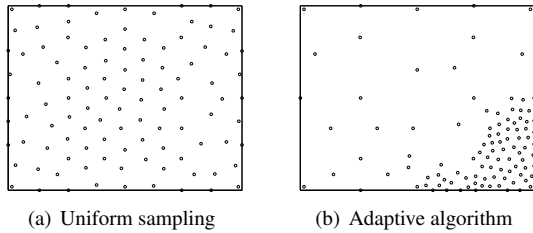


Fig. 4. Distribution of sampling sites.

### 3.2. Piecewise-Constant Field

The next simulation is conducted on a piecewise-constant field, which consists of two constant regions separated by a curvy edge as depicted in Fig. 5(a), which also shows the distribution of sampling sites based on the adaptive method. Fig. 5(b) plots the reconstructed field. As we can see from the artificial ripples in Fig. 5(b) that the thin plate spline interpolation is not suited for reconstructing such piecewise constant fields with sharp edges. However, the sample distribution in Fig. 5(a) shows the remarkable ability of the adaptive algorithm to detect and follow the edge.

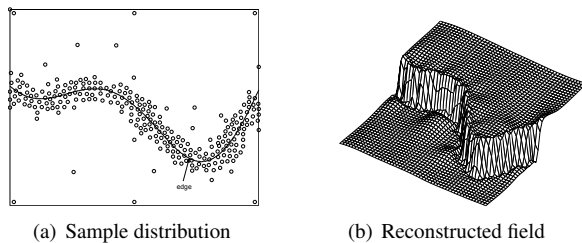


Fig. 5. Adaptively sampling a piecewise-constant field.

## 4. CONCLUSION

In this paper, we developed an algorithm for adaptively sampling and reconstructing two dimensional distributed field, and simulations show that the method works effectively. The routing cost of mobile sensors is not considered in this paper, but it can enter the scheme in various ways. A route design step can be inserted before the sampling takes place. Alternatively, we can incorporate the routing into our sample-selection cost function such that the chance of selecting distant sites in the same iteration is reduced. Although our scheme is designed for individual mobile sensors, it can be used in static sensor networks, if local reconstruction methods are used. For example, a Delaunay triangulation can be easily constructed out of  $DT(S)$ . We can then treat each Delaunay

triangle as a local cluster, and fit a two-dimensional piecewise linear function in it. In addition, there are alternative ways to approximate the Bayesian procedure, and we expect that other iterative schemes can be inspired from the same framework.

## 5. REFERENCES

- [1] M. Rahimi et al., "Adaptive sampling for environmental robotics," in *IEEE Int. Conf. on Robotics and Automation*, New Orleans, USA, 2004.
- [2] R. Nowak, U. Mitra, and R. Willett, "Estimating inhomogeneous fields using wireless sensor networks," *IEEE JSAC*, vol. 22, no. 6, pp. 999–1006, 2004.
- [3] V. Fedorov, *Theory of Optimal Experiments*, Academic Press, London, UK, 1972.
- [4] E. Rafajlowicz, "Optimum choice of moving sensor trajectories for distributed-parameter system identification," *Int. J. Control*, vol. 43, no. 5, pp. 1441–51, 1986.
- [5] P. Hall and I. Molchanov, "Sequential methods for design-adaptive estimation of discontinuities in regression curves and surfaces," *Annals of Statistics*, vol. 31, no. 3, pp. 921–941, 2003.
- [6] M. Batalin et al., "Call and response: experiments in sampling the environment," in *Proc. of ACM Sensys*, Baltimore, USA, Nov 2004.
- [7] D. Donoho, "Compressed sensing," *IEEE Trans. Inf. Theory*, vol. 52, no. 4, pp. 1289–1306, 2006.
- [8] R. Castro, J. Haupt, and R. Nowak, "Faster rates in regression via active learning," in *Neural Information Processing Systems (NIPS)*, 2005.
- [9] F. Aurenhammer and R. Klein, "Voronoi diagrams," in *Handbook of Computational Geometry, Chapter V*, J. Sack and G. Urrutia, Eds., pp. 201–290. Elsevier Science Publishing, 2000.
- [10] M. Johnson, L. Moor, and D. Ylvisaker, "Minimax and maximin distance designs," *J. Stat. Plan. and Infer.*, vol. 26, no. 2, pp. 131–148, Oct. 1990.
- [11] F. Bookstein, "Principal warps: thin-plate splines and the decomposition of deformations," *IEEE Trans. Pattern Analysis and Machine Intelligence*, vol. 11, no. 6, pp. 567–585, June 1989.
- [12] Grace Wahba and Ron Rozier, *Spline Models for Observational Data*, Cambridge University Press, 1990.
- [13] M. Caldwell and R. Percy, *Exploitation of Environmental Heterogeneity by Plants: Ecophysiological Processes Above- and Belowground*, Academic Press, 1994.